Journal of Food Engineering 93 (2009) 89–100

Contents lists available at ScienceDirect

Journal of Food Engineering

journal homepage: www.elsevier.com/locate/jfoodeng

Scale up and design of processes in aerated-stirred fermenters for the industrial production of vinegar

José-María González-Sáiz [a,*], Diego Garrido-Vidal [a], Consuelo Pizarro [b]

[a] Chemical Engineering, Department of Chemistry, University of La Rioja, C/Madre de Dios 51, 26006 Logroño, La Rioja, Spain
[b] Analytical Chemistry, Department of Chemistry, University of La Rioja, C/Madre de Dios 51, 26006 Logroño, La Rioja, Spain

ARTICLE INFO

Article history:
Received 8 September 2008
Received in revised form 29 November 2008
Accepted 6 January 2009
Available online 20 January 2009

Keywords:
Desirability function
Fermentation
Genetic algorithms
Scale up
Simulation environment
Vinegar production

ABSTRACT

A scale-up methodology was applied to the model previously developed for the industrial production of vinegar in an aerated-stirred pilot fermenter. The response surfaces generated by the model demonstrated that aerated mechanical power input, superficial air velocity, temperature, hydrostatic pressure and concentrations of compounds must be kept in the industrial-scale fermenters with the same geometry dimensions as the pilot fermenter. These variables maintain the values of k_La, $C^*_{O_2,L}$ and OTR_{max} and asses the same effects of hydrodynamics and oxygen transfer, allowing the values of the process variables of the industrial-scale fermenters to be scaled down to the values of the pilot fermenter, which are required for applying the models. On these bases, a Simulation Environment for Acetification Processes (SEAP) was developed to design industrial processes on any scale and to predict the behaviour of fermentations and the costs of vinegar production. Finally, an example of the design and optimisation of a fermentation process with SEAP is reported, applying an optimisation methodology based on response surfaces and genetic algorithms using a desirability function as the response.

1. Introduction

Bioreactor process variables affect cell growth by influencing metabolic pathways and changing intracellular reaction rates. A previous study (Garrido-Vidal et al., 2003) examined the effect of hydrostatic pressure, ethanol concentration, aeration, agitation and temperature, i.e. the process variables of an aerated-stirred fermenter, on the acetification rate. The authors then modelled the oxygen transfer, the liquid–gas transfers of volatile compounds and the industrial production of vinegar in aerated-stirred fermenters with these process variables (González-Sáiz et al., 2008, 2009).

When a model is developed and the fermentation is controlled at pilot scale, the most important challenge for the biotechnologist is the scale up of the process, which transfers the models and the results obtained in the pilot plant to the industrial-scale fermenter. Scale up has been studied in depth in industrial fermentation processes, as reported by Schmidt (2005). However, it has not been studied in such depth in acetic fermentation, where it has not been demonstrated that the kinetic models proposed in literature may be applied in industrial-scale fermenters.

Scale-up affects the environment of microorganisms through parameters such as nutrient availability, pH, temperature, dissolved oxygen concentration, shear conditions and foam production (Aiba et al., 1973). These parameters are related to the hydrodynamics of the medium and oxygen transfer. The critical point of the scale-up methodology is the identification of the parameters which must be kept constant between the pilot scale and the industrial-scale fermenter, in order to replicate the same environmental conditions. A perfect replication is impossible, so different scale-up strategies have been proposed. The parameters used most in agitated and aerated processes have been described in specific handbooks, such as Perry's et al. (2001) and Vogel and Todaro's (1997), and extensively reported by Schmidt (2005). Since the acetic fermentation model developed previously by the authors contains the effects of oxygen transfer and hydrodynamics on cell growth, the first objective of this study was to demonstrate the applicability of the model through a scale-up strategy to predict fermentation processes in aerated-stirred fermenters geometrically scaled from the pilot fermenter.

A simulation environment with a good predictive ability is a very useful tool for evaluating, designing and optimising bioprocesses, and for proposing control strategies, once the kinetic models, reactor model and transfer models have been developed. Simulation environments have been developed and applied to different biosystems, and several examples can be highlighted, such as Cramer et al. (2001), Lee et al. (2007) and Shukla et al. (2005). Focusing on vinegar, simulation environments have been applied to different kinetic models and fermentation systems,

* Corresponding author. Tel.: +34 941299634; fax: +34 941299621.
E-mail address: josemaria.gonzalez@unirioja.es (J.-M. González-Sáiz).

0260-8774/$ - see front matter © 2009 Elsevier Ltd. All rights reserved.
doi:10.1016/j.jfoodeng.2009.01.002

Nomenclature

A	acetic acid concentration in the bioreactor and in the effluent stream, g L^{-1}
A_f	acetic acid concentration in wine, g L^{-1}
A_{ic}	external area of the internal coil, m^2
AMC	acethyl methy carbinol (Acetoin) concentration in the bioreactor and in the effluent stream, g L^{-1}
AMC_f	acethyl methy carbinol (Acetoin) concentration in wine, g L^{-1}
B	number of blades on impeller
$C^*_{i,L}$	concentration of component i in liquid phase before mass transfer, g L^{-1}
Ci	concentration of component i in fermentation medium and effluent stream
$C_{O_2,L}$	concentration of oxygen in liquid phase, g L^{-1}
$C^*_{O_2,L}$	concentration of oxygen in oxygen-saturated liquid phase, in equilibrium with partial oxygen pressure in the oxygen-saturated gas phase, g L^{-1}
$C_{P,L}$	heat capacity of fermentation medium, kcal kg^{-1} °C^{-1}
$C_{P,L}$	heat capacity of fermentation medium, kcal kg^{-1} °C^{-1}
$C_{P,w}$	heat capacity of cooling water, Kcal kg^{-1} °C^{-1}
D	impeller diameter, m
D_F	diameter of the pipe (charge, discharge or internal coil) in Fanning Equation, m
D_i	internal diameter of the internal coil pipe, m
D_{Li}	internal impeller diameter, m
$\overline{D_L}$	log mean diameter of the internal coil, $\overline{D_L} = \frac{D_o - D_i}{\ln\left(\frac{D_o}{D_i}\right)}$, m
D_o	external diameter of the internal coil pipe, m
D_S	sparger diameter, m
D_{SP}	diameter of the sparger pipe, m
D_V	vessel diameter, m
E	ethanol concentration in the bioreactor and in the effluent stream, g L^{-1}
E_f	ethanol concentration in wine, g L^{-1}
EA	ethyl acetate concentration in the bioreactor and in the effluent stream, g L^{-1}
EA_f	ethyl acetate concentration in wine, g L^{-1}
Fwater	cooling water flow along the internal coil, m^3 h^{-1}
F_V	volumetric flow rate of vinegar effluent stream (L h^{-1})
g	gravitational constant, 9.8 m s^{-2}
H_B	baffle height, m
H_C	height of the charge point, m
H_{base}	height of the base, m
H_d	height of the discharge point, m
H_F	Friction loss factor contribution in Bernoulli's equation, m
h_i	individual internal heat transfer, kcal m^{-2} °C^{-1} h^{-1}
H_{I1}	height of impeller 1, m
H_{I2}	height of impeller 2, m
H_m	ungassed liquid medium height, m
H_{mg}	gassed liquid medium height, m
h_O	individual external heat transfer, kcal m^{-2} °C^{-1} h^{-1}
H_o	hold-up of air bubbles, %
H_s	sparger height, m
H_T	fermenter vessel height, m
H_{top}	height of the dished top, m
J	baffle width, m
$k^a_{A,G}$	volumetric acetic acid transfer coefficient in gas-side interphase, h^{-1}
$k^a_{AMC,G}$	volumetric acetoin transfer coefficient in gas-side interphase, h^{-1}
$k^a_{E,G}$	volumetric ethanol transfer coefficient in gas-side interphase, h^{-1}
$k^a_{EA,G}$	volumetric ethyl acetate transfer coefficient in gas-side interphase, h^{-1}
$k^a_{i,G}$	volumetric component i transfer coefficient in gas-side interphase, h^{-1}
$k^a_{W,G}$	volumetric water transfer coefficient in gas-side interphase, h^{-1}
k^a_L	volumetric oxygen transfer coefficient in liquid-side interphase, h^{-1}
k_L	thermal conductivity of fermentation medium $\frac{\text{kcal}}{\text{m h °C}}$
k_m	thermal conductivity of stainless steel, 46 $\frac{\text{kcal}}{\text{m h °C}}$
k_W	thermal conductivity of water $\frac{\text{kcal}}{\text{m h °C}}$
L	length of the blades, m
L_B	baffle length, m
L_F	length of the pipe (charge, discharge or internal coil) in Fanning's Equation, m
$LGTR_i$	liquid–gas transfer rate for component i, g L^{-1} h^{-1}
N	impeller rotation speed, rpm or s^{-1}
N_P	power number
n_r	number of Rushton turbines
N_{loops}	number of loops of the internal coil
op	overpressure obtained with pressure valve of fermenter, atm
OTR	oxygen transfer rate
OTR_{max}	maximum oxygen transfer rate
OUR	oxygen uptake rate
P	pressure in fermentation medium, atm
p_a	atmospheric pressure, atm
$p_{H_2O,T}$	water vapour pressure at temperature T, atm
P_g	aerated mechanical power input, W
P_o	non-aerated mechanical power input, W
Q_S	volumetric gas flow rate through liquid medium, m^3 s^{-1}, dm^3 h^{-1}
Q_T	heat transferred to the fermentation medium, kcal
Q_{T_O}	heat taken out by the internal coil from the fermentation medium, kcal
r	recycling rate
R	number of baffles
r_A	acetic acid production rate due to the fermentation process, g L^{-1} h^{-1}
r^2A	adjusted correlation rate
r_{AMC}	acethyl methy carbinol (acetoin) formation rate due to the fermentation process, g L^{-1} h^{-1}
r_{EA}	ethyl acetate formation rate due to the fermentation process, g L^{-1} h^{-1}
r_E	ethanol consumption rate due to the fermentation process, g L^{-1} h^{-1}
R_e	Reynolds number, $\frac{\rho_L N D^2}{\eta_L}$
r_i	rate of production or consumption of component i within the fermenter, g L^{-1} h^{-1}
r_{O_2}	oxygen consumption rate due to the fermentation process, g L^{-1} h^{-1}
r_{X_t}	cell growth rate due to the fermentation process, g L^{-1} h^{-1}
SM	suspended matter concentration in the bioreactor and in the effluent stream, gDW L^{-1}
SM_f	suspended matter concentration in wine, gDW L^{-1}
T_i	input temperature of cooling water, °C
T_L	liquid phase temperature, °C or K
T_O	output temperature of cooling water, °C
T_{wine}	wine temperature, °C or K
U_O	overall heat transfer coefficient, referred to the external area, kcal m^{-2} °C^{-1} h^{-1}
u_F	linear velocity if the fluid (cooling water, wine or gassed medium) in Fanning's equation, m s^{-1}
u_W	linear velocity of the cooling water along the internal coil, m s^{-1}

V_G	gas phase volume, dm^3, m^3
V_{LG}	ungassed liquid phase volume, dm^3, m^3
V_L	gassed liquid phase volume, dm^3, m^3
vvm	air-flow rate divided by the reactor working volume, measured at the exhaust line of the fermenter at 25 °C and 1 atm, h^{-1}
V_c	volume of wine charged, L
V_d	volume of ungassed fermentation medium discharged, L
$V_{d,g}$	volume of gassed fermentation medium discharged, L
W	width of the impeller blades, m
x	thickness of the internal coil, $x = \frac{D_o - D_i}{2}$, m
X	factors of the quadratic model
X_t	total biomass concentration in the bioreactor and in the effluent stream, gDW L^{-1}
$X_{t,f}$	total biomass concentration in wine, gDW L^{-1}
$Y_{A/E}$	acetic acid/ethanol stochiometric coefficient (1.30 g acetic acid/g ethanol)
$Y'_{A/E}$	acetic acid/ethanol yield factor (g acetic acid/g ethanol)
$Y'_{AMC/X}$	acetoin/biomass yield factor (g acetoin/g biomass)
$Y_{A/O}$	acetic acid/oxygen stoichiometric coefficient (1.88 g acetic acid/g oxygen)
$Y'_{A/O}$	acetic acid/oxygen yield factor (g acetic acid/g oxygen)
$Y_{EA/A}$	ethyl acetate/acetic acid stoichiometric coefficient (1.47 g ethyl acetate/g acetic acid)
$Y_{EA/E}$	ethyl acetate/ethanol stoichiometric coefficient (1.91 g ethyl acetate/g ethanol)
$Y'_{EA/X}$	ethyl acetate/biomass yield factor (g ethyl acetate/g biomass)
$Y_{E/O}$	ethanol/oxygen stoichiometric coefficient (1.44 g ethanol/g oxygen)
$Y'_{E/O}$	ethanol/oxygen yield factor (g ethanol/g oxygen)
$Y'_{X/E}$	biomass/ethanol yield factor (g biomass/g ethanol)
$Y'_{X/O}$	biomass/oxygen yield factor (g biomass-/g oxygen)

Greek symbols

$\Delta\bar{T}_L$	log mean temperature difference, $\overline{\Delta T_L} = \frac{(T_L - T_O) - (T_L - T_i)}{\ln\frac{(T_L - T_O)}{(T_L - T_i)}}$, °C
Φ	economical cost, €/° L of acetic acid
f	Fanning friction factor, a dimensional
ε	surface roughness of the pipe, m
$\mu_g v$	total biomass specific growth rate, h^{-1}
μ_g	overall specific growth rate, h^{-1}
η_L	liquid medium viscosity, kg m^{-1} s^{-1}
$\eta_{L,g}$	gassed liquid medium viscosity, kg m^{-1} s^{-1}
$\eta_{L,w}$	liquid medium viscosity at temperature of the wall of the internal coil, $\frac{T_L + (T_O + T_i)\cdot 0.5}{2}$, kg m^{-1} s^{-1}
η_W	water viscosity at mean temperature of the cooling water, $(T_O - T_i)\cdot 0.5$, kg m^{-1} s^{-1}
$\eta_{W,w}$	water viscosity at temperature of the wall of the internal coil, $\frac{T_L + (T_O + T_i)\cdot 0.5}{2}$, kg m^{-1} s^{-1}
μ_o	superficial air velocity measured at the exhaust line of the fermenter at 25 °C and 1 atm, h^{-1}, m s^{-1}
μ_S	superficial air velocity through the liquid medium, m s^{-1}
ρ_A	acetic acid density, kg m^{-3}
ρ_E	ethanol density, kg m^{-3}
ρ_L	liquid medium density, kg m^{-3}
$\rho_{L,g}$	gassed medium density, kg m^{-3}
ρ_W	water density at mean temperature of the cooling water, $(T_O - T_i)\cdot 0.5$, kg m^{-3}
ρ_{wine}	wine density, kg m^{-3}
v	viability factor
π	PI number
$\frac{1}{\Psi}$	correction factor over f due to the heat transfer

such as Macías et al. (1996, 1997) and Park and Toda (1990). Nishiwaki and Dunn (2005) applied a previous mechanistic model of acetic fermentation with cell recycling (Park and Toda, 1990) to study, by means of simulation, the steady-state performance of a two-stage cell-recycle bioreactor. A recent work (Jiménez-Hornero, 2007) has developed a simulation environment for acetic fermentation in an autoaspirant pilot fermenter. However, a simulation environment has not been proposed for predicting the evolution of fermentation processes for different arrangements and dimensions of industrial-scale aerated-stirred fermenters, including the prediction of quality and economic variables. The development of this Simulation Environment for Acetification Processes (SEAP) became the second objective of this study.

2. Materials and methods

2.1. Model applied for production of vinegar

In a previous study (González-Sáiz et al., 2009), the total biomass specific growth rate, $\mu_g v$, was modelled by a secondary order polynomial applied to the process variables. The parameter $\mu_g v$ was developed to simultaneously explain the multiplication rate of *Acetobacter aceti* and the fraction of growing biomass. The total biomass concentration, X_t, and the total biomass specific growth rate, $\mu_g v$, explained the growth rate:

$$X_t \cdot v \xrightarrow{\frac{dX_t}{dt}} X_t \tag{1}$$

$$\frac{dX_t}{dt} = \mu_g v \cdot X_t \tag{2}$$

$$\begin{aligned}\mu_g v = {} & 0.06874 - 0.005261 \cdot X_1 + 0.043798 \cdot X_2 + 0.03401 \\ & \cdot X_3 + 0.031077 \cdot X_4 - 0.000232 \cdot X_5 - 0.000595 \cdot X_1 \\ & \cdot X_1 - 0.025606 \cdot X_2 \cdot X_2 - 0.040034 \cdot X_3 \cdot X_3 \\ & - 0.038633 \cdot X_4 \cdot X_4 - 0.009619 \cdot X_5 \cdot X_5 - 0.0077 \cdot X_1 \\ & \cdot X_2 - 0.02373 \cdot X_1 \cdot X_3 + 0.044161 \cdot X_2 \cdot X_3 \\ & - 0.013122 \cdot X_1 \cdot X_4 + 0.031656 \cdot X_2 \cdot X_4 + 0.009065 \\ & \cdot X_3 \cdot X_4 + 0.011637 \cdot X_1 \cdot X_5 - 0.022271 \cdot X_2 \cdot X_5 \\ & - 0.017904 \cdot X_3 \cdot X_5 + 0.011003 \cdot X_4 \cdot X_5\end{aligned} \tag{3}$$

where X_1, X_2, X_3, X_4 and X_5 were the codified values for the process variables:

$$X_1 = \frac{P - 1.5}{0.5} \tag{4}$$

$$X_2 = \frac{E - 20.681}{27.39} \tag{5}$$

$$X_3 = \frac{\text{vvm} - 19.917}{20.084} \tag{6}$$

$$X_4 = \frac{N - 600}{505.9} \tag{7}$$

$$X_5 = \frac{T_L - 29.5}{4.52} \tag{8}$$

Codification prevented variables with large figures from becoming more important, concealing other variables. The adjusted correlation rate value, 0.984, demonstrated the suitability of the quadratic model. The individual and combined effects of the process variables were explained previously by biological and physico-chemical arguments (Garrido-Vidal et al., 2003). Substrate consumption (i.e. ethanol and oxygen), main product synthesis

Table 1
Yield factors.

Yield factor	Value
$Y'_{A/E}$	1.29 ± 0.02
$Y'_{A/O}$	1.9 ± 0.2
$Y'_{E/O}$	1.5 ± 0.1
$Y'_{X/E}$	0.0061 ± 0.0006
$Y'_{X/O}$	0.009 ± 0.001
$Y'_{EA/X}$	6.6 ± 0.7
$Y'_{AMC/X}$	2.2 ± 0.3

(i.e. acetic acid) and secondary compounds production (i.e. acetoin and ethyl acetate) were related to the growth rate by a growth associated kinetic:

$$r_E = \left(-\frac{1}{Y'_{X/E}}\right)\cdot \mu_g v \cdot X_t \tag{9}$$

$$r_{O_2} = \left(-\frac{1}{Y^{E/o}}\frac{1}{Y'_X/E}\right)\cdot \mu_g v \cdot X_t \tag{10}$$

$$r_A = Y_{A/E}\cdot\frac{1}{Y'_{X/E}}\mu_g v \cdot X_t \tag{11}$$

$$r_{EA} = Y'_{EA/X}\cdot \mu_g v \cdot X_t \tag{12}$$

$$r_{AMC} = Y'_{AMC/X}\cdot \mu_g v \cdot X_t \tag{13}$$

The values of the yield factors are shown in Table 1. The 95% interval confidence of the experimental yield factors $Y'_{A/E}$, $Y'_{E/O}$, and $Y'_{A/O}$ included the values of the respective stoichiometric coefficients $Y_{A/E}$, 1.30 g/g, $Y_{E/O}$, 1.44 g/g and $Y_{A/O}$, 1.88 g/g.

The dissolved oxygen concentration was described by the balance between the oxygen transfer rate (*OTR*) and the oxygen uptake rate (*OUR*):

$$\frac{dC_{O_2,L}}{dt} = k_L a\cdot\left(C^*_{O_2,L} - C_{O_2,L}\right) - r_{O_2} \tag{14}$$

The concentration of oxygen in oxygen-saturated fermentation medium, $C^*_{O_2,L}$, the volumetric oxygen transfer coefficient, $k_L a$, and the liquid–gas transfers were modelled in a previous study (González-Sáiz et al., 2008):

$$C^*_{O_2,L} = e^{\left(1579.2\cdot\frac{1}{(T_L+273.15)}-3.1794\right)}\cdot\frac{p-p_{H_2O,T_L}}{1-p_{H_2O,T_L}} \tag{15}$$

$$N_P = \frac{P_o\cdot g}{\rho_L\cdot N^3\cdot D^5} = 336.5\left(\frac{W}{D}\right)\left(\frac{L}{D}\right)^{1.5}\left(\frac{J}{D}\right)^{0.3}\left(\frac{B}{6}\right)^{0.56}\left(\frac{R}{4}\right)^{0.4} \tag{16}$$

$$Q_S = \frac{\text{vvm}}{3600}\cdot V_L\cdot\frac{T_L+273.15}{25+273.15}\cdot\frac{1}{p} \tag{17}$$

$$\mu_s = Q_S\cdot\frac{1}{\pi\cdot D_V^2\cdot 0.25} \tag{18}$$

$$P_g = P_o\cdot 0.1\cdot\left(\frac{N^2\cdot D^4}{g\cdot W\cdot V_L^{2/3}}\right)^{-1/3}\left(\frac{Q_s}{N\cdot V_L}\right)^{-1/4} \tag{19}$$

$$k_L a = 1.0386\cdot 10^4\cdot(1.319)^p\cdot(1.107)^{T_L}\cdot\left(\frac{P_g}{V_L}\right)^{0.363}\cdot(\mu_s)^{1.439} \tag{20}$$

$$LGTR_i = k_{i,G}a\cdot C^*_{i,L} \tag{21}$$

$$\text{Ethyl acetate: } k_{EA,G}a = 565.2\cdot(0.3730)^p\cdot(1.008)^{T_L}\cdot\left(\frac{P_g}{V_L}\right)^{0.019}\cdot(\mu_s)^{1.106} \tag{22}$$

$$\text{Ethanol: } k_{E,G}a = 0.590\cdot(0.4346)^p\cdot(1.060)^{T_L}\cdot\left(\frac{P_g}{V_L}\right)^{0.030}\cdot(\mu_s)^{0.910} \tag{23}$$

$$\text{Acetoin: } k_{AMC,G}a = 0.061\cdot(0.6006)^p\cdot(1087)^{T_L}\cdot\left(\frac{P_g}{V_L}\right)^{0.154}\cdot(\mu_s)^{1.251} \tag{24}$$

$$\text{Acetic acid: } k_{A,G}a = 0.173\cdot(0.5126)^p\cdot(1.087)^{T_L}\cdot\left(\frac{P_g}{V_L}\right)^{0.167}\cdot(\mu_s)^{1.404} \tag{25}$$

$$\text{Water: } k_{W,G}a = 0.892\cdot(0.3028)^p\cdot(1.070)^{T_L}\cdot\left(\frac{P_g}{V_L}\right)^{0.102}\cdot(\mu_s)^{1.335} \tag{26}$$

where $C^a_{O_2,L}st$ and $C^a_{i,L}st$ were expressed in g/L, $k_L a$ and $k_{i,G}a$ in h^{-1}, p and p_{H_2O} in atm, T_L in °C, P_g in W; V_L in m^3 and μ_S in m s^{-1}. Superficial air velocity measured at the exhaust line of the fermenter had to be corrected for the effect of pressure and temperature of the medium on air flowing through the fermentation medium, to calculate μ_S The parameters of the models were calculated using the data obtained with a New Brunswick (BioFlo IV) pilot fermenter, with a maximum working volume of 10 L. The details of the pilot fermentation system, the experiments and the analytical methods were described in previous studies (Garrido-Vidal et al., 2004; González-Sáiz et al., 2008, 2009). The models can be applied within the ranges of process variables and concentrations shown in Table 2. The concentration ranges of the other parameters analysed in the fermentation medium, i.e., acetic acid, ethyl acetate, acetoin and suspended matter have been also reported in Table 2. These parameters can be considered as system responses because they depend on wine concentration and fermentation kinetics. In fact, acetic acid is stoichiometrically related to ethanol concentration. The models developed for $k_L a$ and $k_{A,G}a$ and were based on variables which depended on the process variables, vessel geometry and the design of the agitation and aeration system and can therefore be applied in any fermenter with the same aeration and agitation system design and the same geometry dimension rates as the pilot fermenter. Table 3 shows the geometric dimensional similarities that must be kept in the large-scale fermenters in order to apply these transfer models.

2.2. Computational methods

The Simulation Environment for Acetification Processes was programmed in Matlab 7.3.0.267 R2006b (The MathWorks Inc.). The response surfaces studied in Section 3.1. were built using the same software.

The optimisation methodology reported in Section 3.3 consisted in applying a desirability function (Massart et al., 1994) to the responses selected for optimisation. The desirability function was maximized using a genetic algorithm programmed in Matlab 7.3.0.267 R2006b (The MathWorks Inc.). Each chromosome was built with values of the process variables, and the desirability function responses were calculated using the second order polynomial models provided by NEMROD-W version 9901. These models were

Table 2
Range of process variables and concentrations used in the models.

Variable	Range
Pressure	1–2 atm
Ethanol concentration	1–50 g/L
Acetic acid concentration	57–132 g/L
Ethyl acetate concentration	0.02 – 4 g/L
Acetoin concentration	0.75–1.50 g/L
Suspended matter	0.24–0.94 g/L
vvm	3–37 h^{-1}
μ_o	1.91×10^{-4}–2.36×10^{-3} m s^{-1}
Agitation	200–1000 rpm
Temperature	26–33 °C

Table 3
Geometric similarities which must be maintained in large-scale fermenters to apply the models developed for the pilot fermenter.

Vessel		Impeller		Baffles		Sparger	
H_T/D_v	2.01	H_{I1}/D_V	0.1816	H_B/D_V	0.2205	H_S/D_V	0.1053
H_m/D_V	1.37	H_{I2}/D_V	1.0211	R	3	D_S/D_V	0.3174
H_{top}/D_V	0.1786	D_V/D	2.3356	J/D	0.267	D_{SP}/D_S	0.0208
H_{base}/D_V	0.4684	D_{LI}/D	0.754	L_B/D	3.3805		
H_C/H_{top}	0.5	W/D	0.2090				
H_d/H_{base}	1	L/D	0.2581				
		B	6				
		n_r	2				

calculated previously by a Doehlert design (Doehlert, 1970; Massart et al., 1994) applied to the process variables and the responses were obtained from the simulation results provided by SEAP. This methodology economized computational time.

The genetic algorithm was developed from the basic genetic algorithm (Lucasius and Kateman, 1993, 1994) and had been applied previously by the authors in modelling (Gonzaléz-Saiz et al., 2008). The features of the algorithm were described in González-Sáiz et al. (2008).

3. Results and discussion

3.1. Scale up of the model

Fig. 1 shows the response surfaces of $\mu_g v$ vs. ethanol concentration and OTR_{max}. As explained in Section 2.1, $\mu_g v$ represents the multiplication rate of *Acetobacter aceti* and the fraction of cells which were growing. Since the kinetic of acetic acid production is growth associated, the effects of the substrates and the process variables on $\mu_g v$ were critical for designing a scale-up methodology. OTR_{max} is the maximum oxygen transfer rate provided by a set of process variables, regarding Eq. (14):

$$OTR_{max} = k_L a \cdot C^*_{O_2,L} \tag{27}$$

OTR_{max} represents the oxygen transfer ability of the biosystem, which is one of the most process-relevant parameter in an aerobic process. In acetic fermentation, the effects of oxygen concentration on bacterial growth have traditionally been considered when, from a physical standpoint, it is more adequate to use the oxygen transfer rate since dissolved oxygen is a response on the part of the system due to the balance between the Oxygen Uptake Rate and the Oxygen Transfer Rate. The oxygen transferred to the medium, which is represented by OTR_{max}, and ethanol, are the substrates required by *Acetobacter aceti* to produce acetic acid.

The OTR_{max} values were obtained by a full combination of 9, 5 and 5 levels of agitation, aeration and ethanol, respectively. Each response surface was obtained at constant pressure and temperature. The response surfaces were built with Matlab 7.3.0.267 R2006b (The MathWorks Inc.), applying the models reported in Section 2.1.

The shape of the curves for ethanol and oxygen transfer were very similar, i.e. very low levels of ethanol or oxygen made the acetification rate decrease and a saturation effect with high levels of oxygen or ethanol was observed. This saturation effect increased

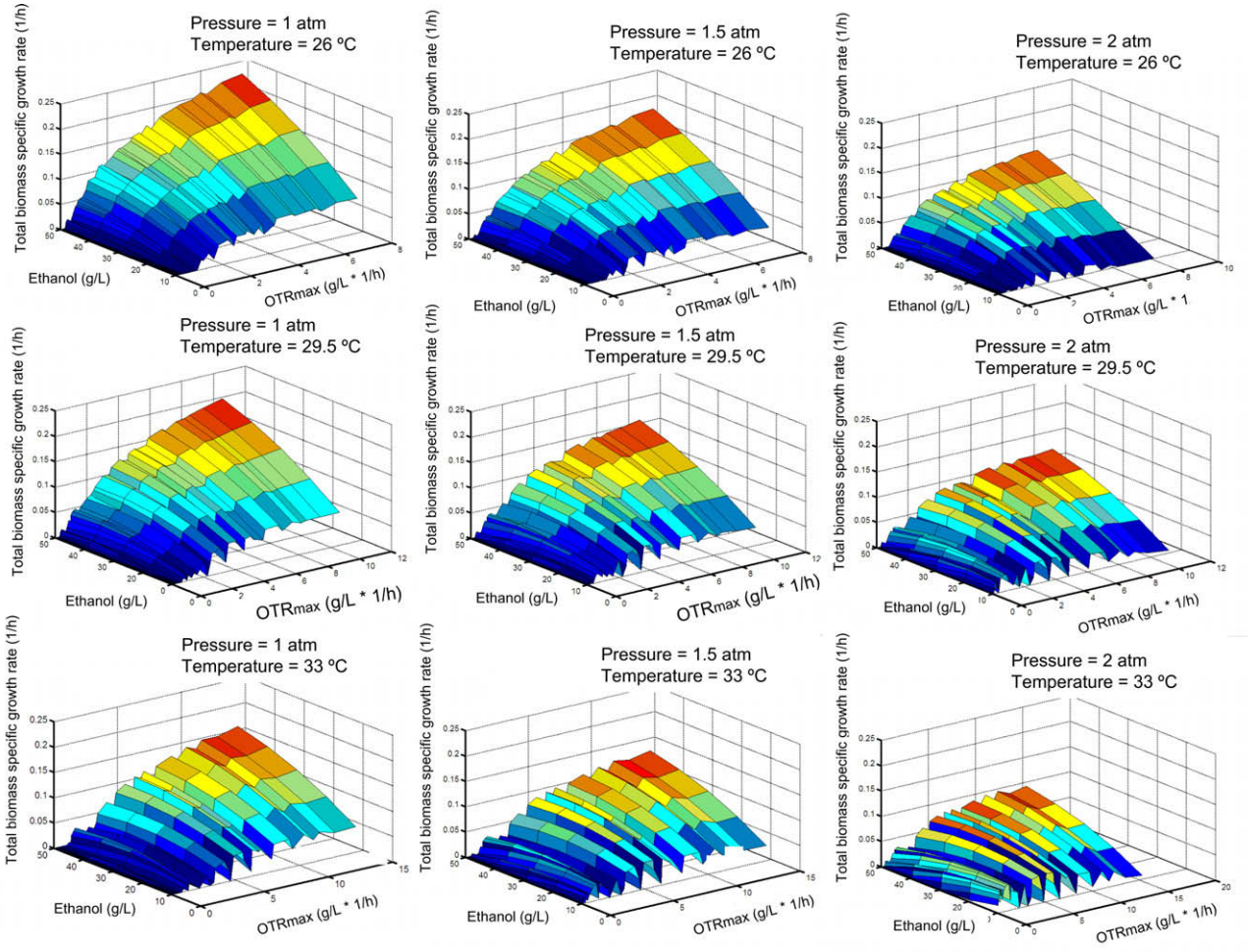

Fig. 1. Response surfaces for $\mu_g v$ vs. ethanol concentration and OTR_{max}.

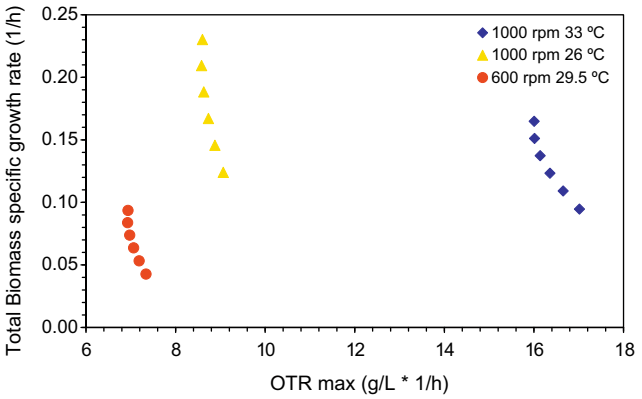

Fig. 2. Plots of $\mu_g v$ vs. OTR_{max} at 37 vvm and 50 g/L and different agitation speed and temperature values. OTR_{max} in each plot was varied by increasing pressure from 1 atm to 2 atm.

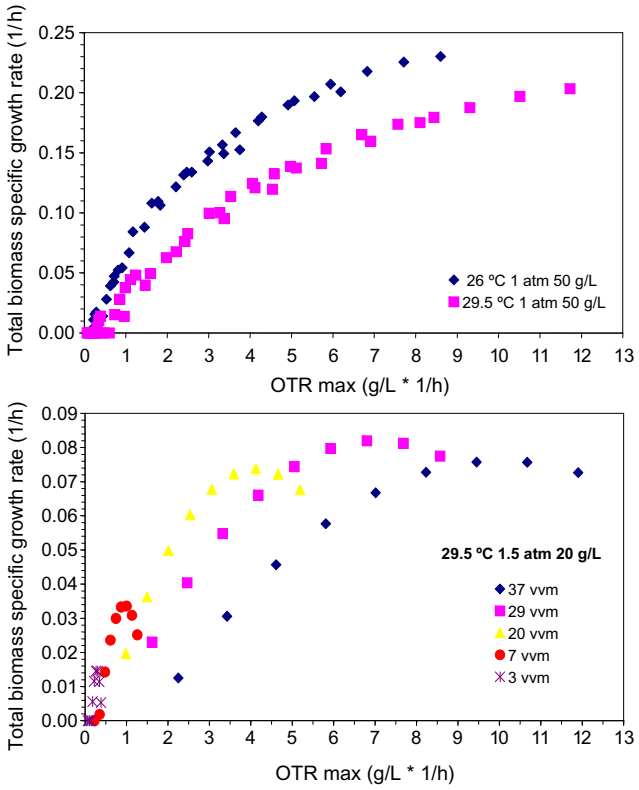

Fig. 3. Plots of $\mu_g v$ vs. OTR_{max} at different hydrostatic pressure, ethanol concentration and temperature: (a) conditions without inhibition due to aeration and agitation and (b) conditions with inhibition.

for oxygen transfer at low levels of ethanol and for ethanol at low levels of oxygen transfer. The response surfaces also displayed the clear inhibitory effect of hydrostatic pressure on $\mu_g v$ and an inhibitory effect of temperature at high levels of ethanol and OTR_{max}. Hydrostatic pressure also increased the inhibitory effects of temperature and ethanol. The saturation effect of ethanol became an inhibitory effect when hydrostatic pressure and temperature were increased. In a previous study (Garrido-Vidal et al., 2003), the effect of pressure was related to the inhibitory effect of oxygen transfer. In that study, the oxygen transfer model had not yet been developed. As regards the results obtained with the oxygen transfer models, Figs. 1 and 2 show that $\mu_g v$ decreased when hydrostatic pressure was enhanced in both high and low ranges of OTR_{max} values; hence, inhibition was due to the direct effect of pressure. However, at high temperature levels and low levels of OTR_{max} and ethanol concentration, hydrostatic pressure had a slightly positive effect on $\mu_g v$, because OTR_{max} increased with pressure due to the enhancement of $C^*_{O_2,L}$ (Eq. (15)) and $k_L a$ (Eq. (20)), and compensated for the inhibitory effect at very low oxygenation conditions. A similar effect was observed with temperature because temperature enhanced $k_L a$ and μ_s.

In case of oxygen transfer, the saturation effect did not turn into an inhibitory effect when temperature and pressure were enhanced. The model for $\mu_g v$ provides that the optimum conditions for the bacterial growth are reached at maximum levels of aeration and agitation and at maximum ethanol concentration. However, the tendency displayed in the figures showed that the inhibitory effects could appear with stronger oxygenation conditions. Fig. 3a shows two examples of saturation curves of $\mu_g v$ vs. OTR_{max}, at constant values of pressure, ethanol and temperature and obtaining the OTR_{max} by combining 9 agitation levels and 5 aeration levels. These curves would correspond to the flat surface areas of the response surfaces in Fig. 1. However, in Fig. 3b, instead of a singular curve a dispersion of plots were obtained. By clustering the points with the same aeration, it was concluded that agitation had an inhibitory effect over 800 rpm and aeration had an inhibitory effect over 20 vvm, independently of the OTR_{max} values. This inhibitory effect explained the valleys and "accordion shape" of the response surfaces in Fig. 1. This type of inhibition is not related to the oxygen transfer and is explained by the shear stress and cell damaged caused by strong agitation and aeration (Brindley Alías et al. 2004; El-Enshasy et al., 2006), and the cell damage caused by collisions with turbulent eddies in the growth medium (Çelik and Çalik, 2004; Papoutsakis, 1991). From Fig. 1 it may be deduced that this inhibitory effect is enhanced at low levels of ethanol concentration and high temperature and hydrostatic pressure levels.

These results demonstrate that ethanol concentration, temperature, pressure and OTR_{max} must be kept constant in industrial-scale fermenters to asses the same behaviour of bacteria as in the pilot fermenter. If pressure and temperature are kept constant, in order to keep constant OTR_{max}, $k_L a$ must be maintained (Eq. (27)) since $C^*_{O_2,L}$ depends on pressure and temperature. Consequently, the dissolved oxygen concentrations should be the same in the industrial-scale fermenters. As hydrostatic pressure and $k_L a$ are kept constant, this scale-up strategy includes the aim of the scale-up factor $k_L a \cdot p$ (Aiba et al., 1973). It has also been shown that agitation and aeration affect $\mu_g v$ independently of oxygen transfer. Superficial air velocity and aerated mechanical power input depend on the geometry of the fermenter and are therefore scaleable variables. If $\frac{P_g}{V_L}$ and μ_S are kept constant, the interfacial area a is maintained constant with the scale. Furthermore, μ_S represents another phenomenon related to aeration, such as flooding and foaming (Aiba et al., 1973) and has been proposed by some authors as the scale-up parameter for a large range of vessel sizes (Vogel and Todaro, 1997). Therefore, μ_S must be also kept constant in industrial-scale fermenters. Once the values of hydrostatic pressure, temperature and μ_S are fixed, the only way to keep the value of $k_L a$ between the scales is by maintaining $\frac{P_g}{V_L}$ constant. The design of the Rushton turbine ensures that most of the motor power is consumed at the tips of the agitator, thus maximizing the energy used for bubble shearing. $\frac{P_g}{V_L}$ is the most used variable parameter for describing mixing in reactors with Rushton turbines and has been mathematically related with other mixing parameters (Wernersson and Trägårdh, 1999). Furthermore, $k_L a$ and $\frac{P_g}{V_L}$ have been reported as the most applied and successful scale-up parameters in aerobic processes, (Aiba et al., 1973; Perry Handbook, 2001; Wong et al., 2002, 2003; Kim et al., 2003; Betts et al., 2006), where oxygen transfer is the limiting factor.

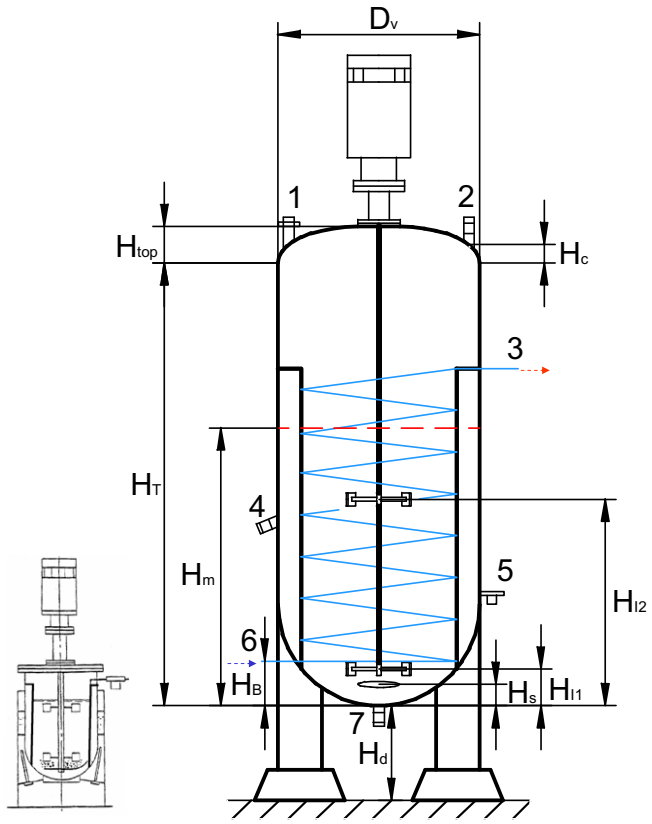

Fig. 4. Diagram of the pilot fermenter vs. the scaled-up fermenter designed by SEAP. 1 = air outlet and pressure valve; 2 = addition port; 3 = cooling water outlet; 4 = sample port; 5 = air inlet; 6 = cooling water inlet and 7 = outlet port.

3.2. Simulation Environment for Acetification Processes (SEAP)

3.2.1. Design of industrial fermenters

The industrial fermenters designed by SEAP are geometrically scaled from the pilot scale fermenter ensuring that the dimensional similarities stated in Table 3 are maintained. Fig. 4 shows a diagram of the pilot fermenter vs the industrial fermenter designed by SEAP. Instead of the plate top of the pilot fermenter, dished tops are proposed for the industrial-scale fermenter since these are more suitable for vessels larger than 500 L (Aiba et al., 1973). The ratio H_{top}/D_V is the same as the dish top of the 1,00,000 L fermenter used for antibiotic production reported by Aiba et al. (1973). The ratio H_{base}/D_V is calculated considering a dimension of 1.5 m for an industrial fermenter with 30,000 L working volume. Gillard and Trägårdh (2003) demonstrated that the model for mixing times for Rushton turbines was independent of the scale and was only affected by the point of addition of liquid into the medium. In the case of the pilot fermenter, the injection point was in the upper part of the tank, so the industrial fermenters are designed with injection at the same point. The agitation and aeration system are the same as in the pilot fermenter: two Rushtons impellers with three baffles and a ring sparger to diffuse the air homogenously into the vessel. The dimension ratios of the Rushton impellers, the baffles and the ring sparger are shown in Table 3, but they are not shown in Fig. 4 for the purpose of clarity.

The industrial fermenter is designed with one helical internal coil. Internal coils are mainly used in industrial-scale fermenters, while water jackets are mostly used in laboratory and pilot-scale fermenters because coils are cheaper to replace than the tank wall and jacket in the event of corrosion and the cost of a fermenter with helical coils is cheaper than a jacketed tank. Helical coils do not affect the agitation of the medium with radial turbines if the spaces between the coil loops are 1–1.5 pipe diameters (Vogel and Todaro, 1997). Luyben (2004) demonstrated that the internal coil cooling provided better dynamic controllability than jacket cooling in terms of being able to handle larger disturbances. The internal coil is designed by SEAP for installation between the baffles and with a vertical length equal to the length of the baffles (Perry et al., 2001). The standardized diameter of the pipe is calculated on the basis of 3″ for a working volume of 13225.4 L. The internal and external diameters are calculated by the USA standard dimension table of steel and ferrous pipes. The loop diameter is 98% of the space between the baffles, representing 75.56% of vessel diameter. The space between the loop flights corresponds to the external diameter of the pipe and the number of loops is:

$$N_{loops} = \frac{L_B}{2 \cdot D_0} \tag{28}$$

These parameters were introduced into SEAP based on Luyben's design (2004) to avoid interferences in mixing due to high pipe volumes, small spacing between loops or small loop diameter, but assessing cooling capability.

In Table 3, the main parameter for the geometrical scale up of the fermenter is vessel diameter. Once vessel diameter is calculated for the working volume selected by the user, the other dimensions are related. The working volume for design purposes is the volume equivalent to 6.5 L in the pilot fermenter, which was the volume used to develop the models reported in Section 2.1 for the pilot fermenter (González-Sáiz et al., 2008, 2009). Since the internal coil takes up volume in the vessel and the section of the coil pipe is proportional to the working volume, SEAP runs an iterative process to calculate D_V and the dimensions of the internal coil.

The scale-up window for each design is determined using the ranges in Table 2 in the case of temperature, compound concentrations and aeration, which is determined by the range of μ_o. In the case of pressure, the weight of the medium column is considered, averaged at the middle of the medium height, assessing that maximum pressure is 2 atm. In Eq. (19), the effect of aeration on P_O depended on $\frac{Q_S}{V_L}$ and it decreased when the scale was enhanced and agitation decreased. Due to this effect, for any agitation in the industrial-scale fermenter, the scaled down value increases with aeration, as shown in Table 4, and, for any agitation value in the

Table 4
Variation of scaled down agitation speed with aeration.

Industrial scale					
Pressure (atm)	1.25	2	1.50	1.25	1.76
Aeration ($L\,h^{-1}$)	8357	45,976	43,485	45,976	83,346
μ_S ($m\,s^{-1}$)	1.67E−04	6.57E−04	7.68E−04	9.22E−04	1.31E−03
Temperature (°C)	29.5	29.5	29.5	29.5	29.5
Agitation (rpm)	74	74	74	74	74
Ethanol (g/L)	29.64	20.68	20.38	40.85	7.302
Suspended matter (g/L)	0.39	0.68	0.69	0.37	0.67
Scaled down agitation (rpm)	531	568	576	585	616

Table 5
Variation of scaled-up agitation speed with aeration.

Pilot scale					
Pressure (atm)	2	1.25	1.5	1.75	1.25
Aeration ($L\,h^{-1}$)	19.5	45	58	137	240.5
μ_S ($m\,s^{-1}$)	9.81E−05	3.54E−04	3.89E−04	7.79E−04	1.91E−03
Temperature (°C)	33	26	33	29.5	29.5
Agitation (rpm)	800	800	800	800	800
Ethanol (g/L)	50	50	50	50	50
Suspended matter(g/L)	0.7	0.7	0.7	0.7	0.7
Scaled-up agitation (rpm)	112	108	107	101	96

pilot fermenter, the scaled-up value decreases with aeration, as shown in Table 5. Therefore, the maximum agitation value in the industrial-scale fermenter is calculated from 1000 rpm agitation in the pilot fermenter, ethanol 1 g/L, suspended matter 6 g/L and maximum aeration conditions, i.e. with μ_o $2.36 \times 10^{-3}\,m\,s^{-1}$, hydrostatic pressure 1 atm and temperature 33 °C. These conditions also give the maximum k_La value. The minimum value is calculated from agitation 200 rpm in the pilot fermenter, ethanol 50 g/L, suspended matter 0 g/L and minimum aeration conditions, i.e. with μ_o $1.91 \times 10^{-4}\,m\,s^{-1}$, hydrostatic pressure 2 atm and temperature 26 °C. These conditions also give the minimum k_La value.

The global maximum agitation value is limited by the power of a 800 kW motor, with 95% gear box efficiency, to avoid extremely high power values for large-scale fermenters.

3.2.2. Main system of differential equations

The core of SEAP is the differential equation system of the models reported in Section 2.1:

$$\frac{dX_t}{dt} = \mu_g v \cdot X_t + \frac{V_c \cdot X_{tf}}{V_L \cdot dt} - (1-r)\cdot\frac{V_d \cdot X_t}{V_L \cdot dt} \tag{29}$$

$$\frac{dSM}{dt} = \mu_g v \cdot X_t + \frac{V_c \cdot SM_f}{V_L \cdot dt} - (1-r)\cdot\frac{V_d \cdot SM}{V_L \cdot dt} \tag{30}$$

$$\frac{dE}{dt} = -r_E - \frac{1}{Y_{EA/E}}\cdot r_{EA} - LGTR_E + \frac{V_C \cdot E_f}{V_L \cdot dt} - \frac{V_d \cdot E}{V_L \cdot dt} \tag{31}$$

$$\frac{dC_{O_2,L}}{dt} = k_La \cdot \left(C^*_{O_{2,L}} - C_{O_{2,L}}\right) - r_{O_2} + \frac{V_C \cdot C_{O_{2f}}}{V_L \cdot dt} - \frac{V_d \cdot C_{O_{2,L}}}{V_L \cdot dt} \tag{32}$$

$$\frac{dA}{dt} = r_A - \frac{1}{Y_{EA/A}}\cdot r_{EA} - LGTR_A + \frac{V_C \cdot A_f}{V_L \cdot dt} - \frac{V_d \cdot A}{V_L \cdot dt} \tag{33}$$

$$\frac{dEA}{dt} = r_{EA} - LGTR_{EA} + \frac{V_C \cdot EA_f}{V_L \cdot dt} - \frac{V_d \cdot EA}{V_L \cdot dt} \tag{34}$$

$$\frac{dAMC}{dt} = r_{AMC} - LGTR_{AMC} + \frac{V_C \cdot AMC_f}{V_L \cdot dt} - \frac{V_d \cdot AMC}{V_L \cdot dt} \tag{35}$$

$$\frac{dV_L}{dt} = -\frac{1}{\rho_W}\cdot LGTR_W \cdot V_L + \frac{V_C}{dt} - \frac{V_d}{dt} \tag{36}$$

The differential equation system is solved by an algorithm based on the Runge–Kutta fourth-order method (Mathews and Kurtis, 1999). In each step of the Runge–Kutta algorithm, k_La, P_g and μ_s are calculated with the process variables selected by the user for the industrial-scale fermenter. Hydrostatic pressure is calculated taking into account overpressure and pressure due to the weight of the fermentation medium column, considering the middle of the medium height as average. The methodology described in Section 3.1 is applied to scale down the process variables and apply the model for $\mu_g v$ solving Eqs. (29)–(36).

The density of the medium is considered to be due mainly to water, ethanol, acetic acid and suspension solids, ruling out contributions from other compounds, which are present in very low concentrations in the fermentation medium. The water density at each temperature is calculated using the equation taken from the CRC Handbook of Chemistry and Physics (Lide and Frederikse, 1995) and ethanol density and acetic acid density at each temperature are calculated from the adjusted correlations calculated from the data taken from Perry's Handbook (Perry et al., 2001).

Viscosities of ethanol, acetic acid and water at each temperature are calculated from the adjusted correlations calculated from the data taken from the CRC Handbook of Chemistry and Physics (Lide and Frederikse, 1995). Total viscosity is calculated using the Lobe correlation (Reid et al., 1987). The correlation parameters were calculated from the viscosities of different concentrations of water–ethanol and water–acetic acid taken from Perry's Handbook (Perry et al., 2001).

The volume variation is calculated by V_c and V_d, together with the effect of water loss due to liquid–gas transfer, ruling out the effects of other losses. The hold up of air bubbles is calculated from the adjusted parameters of the straight line provided by Richards' correlation (Aiba et al., 1973):

$$H_o = \left[\left(\left(\frac{P_O \cdot \frac{1}{745.7}}{V_L}\right)^{0.4}\cdot\left(\mu_S \cdot 3600\right)^{0.5}\right) - 2.37\right]\cdot\frac{1}{0.763} \tag{37}$$

The gassed liquid medium height, H_{mg}, is calculated considering the gassed volume and the volume of the internal coil, by iterations. When the gassed volume covers two impellers, Pg is calculated as two times the power number, N_P (Eqs. (16)–(19)). When it covers only one impeller, P_g is calculated with one N_P, and the rate P_g/V_L is scaled down to the pilot fermenter with 6.5 L and covering two impellers, as in the model calculated for $\mu_g v$. Therefore, prediction ability improves when the medium volume is close to the working volume. When the ungassed volume covers one impeller, P_o in Eq. (37) is calculated with one N_P.

It is mathematically possible to obtain negative values for oxygen and ethanol concentrations, and the simulation is stopped when ethanol is consumed. In the case of oxygen, a negative value indicates that oxygen consumption is higher than the oxygen transfer rate. This situation can be achieved in processes with cell recycling, when the accumulation of biomass exceeds system oxygen transfer capacity. In a real process, the growth cell decreases to reach a state with 0% dissolved oxygen, i.e. a limit-by-oxygen state. It can be inferred that in limit-by-oxygen states, cell population viability decreases because there is no oxygen for all the cells. This effect is simulated by introducing a correction factor on $\mu_g v$, calculated inside the Runge–Kutta algorithm to balance growth cell and oxygen consumption with oxygen transferred to the medium and keep oxygen concentration over zero.

Finally, the signal provided by the oxygen probe is predicted from the $C_{O_{2,L}}$ values, considering that the signal is proportional to oxygen partial pressure in the gas phase in equilibrium with $C_{O_{2,L}}$ and that the 100% signal was calibrated by saturation of the fermentation medium with air at 30 °C and 1 atm.

3.2.3. Energy consumption evaluation

SEAP estimates the theoretical energy consumption of each fermentation process. It has been considered that the main energy consumptions are due to agitation, aeration, cooling and auxiliary charge and discharge pumps. The temperature of the medium, T_L,

is calculated within the Runge–Kutta algorithm by solving the following differential equation, which expresses the heat balance of the fermentation medium:

$$\frac{dV_C}{dt}\cdot 0.001\cdot \rho_{\text{wine}}\cdot C_{P,\text{wine}}\cdot (T_{\text{wine}}-T_L)+\frac{dQ_T}{dt}+\frac{dQ_{TO}}{dt} = V_L\cdot 0.001\cdot \rho_L\cdot C_{P,L}\cdot \frac{dT_L}{dt} \quad (38)$$

The mean approximation is the fact that fermentation medium temperature is considered to be homogenised at T_L for the components of the fermentation medium, liquid, solid and gas. The heat capacities of wine and fermentation medium, $C_{P,\text{wine}}$ and $C_{P,L}$ are calculated proportionally to the mass fraction of ethanol, acetic acid and water, ruling out the contributions of other components. The heat capacities of ethanol, acetic acid and water depending on temperature are calculated using the empirical equations provided by Perry's Handbook (Perry et al., 2001). The heat transferred to the medium, Q_T, is calculated as the sum of two contributions, the heat generated by the cells during the exothermic oxidation of ethanol, 495 kJ/mol (Buchanan and Gibbons, 1984) and the heat transferred to the medium due to agitation:

$$\frac{dQ_T}{dt} = \left[P_g\cdot 0.001\cdot 3600000+Y_{A/E}\cdot\frac{1}{Y'_{X/E}}\mu_g v\cdot X_T\cdot\frac{1}{60.05}\cdot 495000\right]\cdot\frac{1}{4185} \quad (39)$$

When temperature is higher than the temperature set, SEAP calculates the heat that must be extracted from the fermentation medium by the internal coil, Q_{TO}, to maintain the set temperature. If temperature is equal to or lower than the set temperature, then Q_{TO} and the water flow through the internal coil is zero, Q_{TO} is calculated using the general equations for coil heat interchangers, applied in the design of the industrial fermenter:

$$\frac{dQ_{TO}}{dt} = U_O\cdot A_{ic}\cdot \overline{\Delta T_L} \quad (40)$$

$$A_{ic} = \pi\cdot D_O\cdot\left(\frac{H_{mg}-H_B}{2\cdot D_O}\cdot\pi\cdot D_{Li}\right) \quad (41)$$

$$\frac{1}{U_O} = \frac{D_o}{h_i\cdot D_i}+\frac{x\cdot D_o}{k_m\cdot \overline{D_L}}+\frac{1}{h_o} \quad (42)$$

where k_m is a user variable, depending on the material of the internal coil. The internal individual coefficient, h_i, is calculated using the Dittus–Boelter empirical correlation, and Chilton, Drew and Jebens' empirical correlation is applied to calculate the external individual coefficient, h_o (Perry et al., 2001), as is normal for a blade impeller. The linear velocity of the cooling water, u_W, is calculated from the balance:

$$F_{\text{water}}\cdot\rho_w\cdot C_{p,w}\cdot(T_O-T_i) = Q_{\text{exch}} \quad (43)$$

$$F_{\text{water}} = u_W\cdot\pi\cdot D_i^2\cdot 0.25 \quad (44)$$

The input temperature of cooling water, T_i, is a user variable. The thermal conductivity of the fermentation medium is calculated from the values of the thermal conductivities for water (k_W), ethanol and acetic taken from the CRC Handbook of Chemistry and Physics (Lide and Frederikse, 1995) and applying the method developed by Li (Reid et al., 1987). Since F_W, Q_{TO} and T_O are unknown, an iterative methodology is applied. An initial T_O is predicted and the iteration finishes when

$$\left|\frac{dV_C}{dt}\cdot 0.001\cdot\rho_{wine}\cdot C_{P,\text{wine}}\cdot(T_{\text{wine}}-T_L)+\frac{dQ_T}{dt} -\left(V_L\cdot 0.001\cdot\rho_L\cdot C_{P,L}\cdot\frac{dT_L}{dt}\right)+\frac{dQ_{T_O}}{dt}\right|\le 0.01 \quad (45)$$

The total energy consumption of the fermentation process is calculated by solving the following differential equation:

$$\frac{dE_T}{dt} = 1.05\cdot(P_g+P_{\text{cool}}+P_d+P_c)+P_{\text{air}} \quad (46)$$

The power of the air blower used for aeration is estimated using the empirical expression taken from Perry's Handbook (Perry et al., 2001):

$$P_{\text{air}} = 2.72\cdot 10^{-5}\cdot Q_S\cdot\left(p_a+op+\frac{\rho_L\cdot g\cdot(H_m-H_s)}{101325}\right) \quad (47)$$

with Q_s in L h^{-1}. As it is shown in Eq. (48), a gear box efficiency of 95% is considered for the motors of the agitator, the water cooling pump and the charge and discharge pumps. P_{cool}, P_d and P_c, are calculated theoretically by Bernoulli equation, to asses the flows F_W, $\frac{dV_{d,g}}{dt}$ and $\frac{dV_c}{dt}$, and using the parameters of the water cooling, gassed medium and wine, respectively. Diameters of the tubes of charge and discharge and maximum available flows are user variables and lengths are calculated with a 10% of security over the minimum length, considering the points of charge and discharge described in Section 3.2.1. The energy loss due to friction undergone by a Newtonian liquid in a pipe is calculated by the Fanning equation (Perry et al., 2001), applying the correlation proposed by Chen (1979) to calculate the Fanning friction factor f. Surface roughness, ε, is a user variable, which depends on the material of the internal coil and the charge and discharge pipes. In the case of the internal coil, the correction factor over f due to heating of cooling water (Perry et al., 2001) is introduced.

If the charge flow of wine is very low, SEAP calculates the frequency of pulses assessing Reynolds higher than 2000, and evaluates motor consumption. If the medium discharge flow does not require a pump, SEAP calculates the programme of an electro valve in the outlet port to asses the discharge flow. Finally, the maximum limits for the charge pump, discharge pump and cooling water are user variables.

3.2.4. Evaluation of steady state and economical balance

When differences between the medians and the averages of a set of variables over a period of time, in case of continuous processes, or during a number of batches in the case of semi-continuous processes, are below certain limits, the simulation environment considers that a steady or semi-steady state has been reached. The period of time or the number of batches for evaluation of the steady or semi-steady state are selected by the user. The values of the limits, shown in Table 6, are lower than the significant figures of the real variables. In the case of a finisher fermenter, overpressure, agitation and aeration are stopped and discharge begins when difference between median and average of ethanol concentration are less than 10^{-4} during a period of time or when both ethanol concentration and ethanol consumption are less than 3.948 g/L and 0.1 g/L, respectively. In all cases, a maximum simulation time can be introduced by the user.

SEAP calculates the energy consumption and the grade-litres of ethanol consumed per grade-litre of acetic acid produced in the fermenter. Introducing the cost of energy and wine enables the estimation of an economical cost per grade-litre of acetic acid. In the case of a finisher fermenter, consideration is also given to the grade-litres of acetic acid supplied by a continuous or semi-continuous fermenter which are consumed per grade-litre of acetic acid produced.

3.3. Example of design and optimisation of an industrial process with SEAP

As an example of the use of SEAP, a fermentation system was designed with a continuous fermenter connected to two finisher

Table 6
Parameters and limits used by SEAP to evaluate the steady and semi-steady states.

Parameter	Limits	
	Continuous (steady state concentrations and wine and vinegar streams)	Semi-continuous (final batch concentrations and volumes charged and discharged)
Vinegar	10^{-2}	10^{-2}
Wine	10^{-2}	10^{-2}
Acetic acid	10^{-4}	10^{-4}
Total biomass	10^{-5}	10^{-5}
Suspended matter	10^{-5}	10^{-5}
Dissolved oxygen	10^{-2}	10^{-2}
Ethyl acetate	10^{-5}	10^{-5}
Acetoin	10^{-5}	10^{-5}
Ethanol	–	10^{-4}

fermenters, with a working design volume of 30,000 L, vessel diameter of 3.23 m and other dimensions within the rates shown in Table 3 and Section 3.2.1. The internal coil material was standard stainless steel type 304 (18% Cr, 8% Ni), which is used very often in the food industry. The thermal conductivity of this material is 14 kcal m^{-1} h^{-1} $°C^{-1}$, according to technical specifications. The decrease in k_m was considered as negligible within the temperature range of the fermentation processes. The surface roughness value was taken from Perry's Handbook (Perry et al., 2001), i.e. 4.57e−5 m for commercial steel. The proposed charge and discharge pipes were flexible PVC pipes for food use, with interior reinforcement and diameter 0.02 m. Surface roughness was 7e−6, considering technical sheets. The maximum flow of charge and discharge pumps was settled as 66,000 L h^{-1}, a value taken from the technical sheets of peristaltic pumps, very used in wine and vinegar industry. Maximum flow of the water cooling pump was settled as 1000 m^3 h^{-1}, a value taken from the technical sheets of magnetic or centrifugal pumps. Input temperatures of water cooling and wine were assigned to be 10 °C and 15 °C, respectively. It was supposed that the fermenter was not equipped with a volatiles recovery system. Finally, cost of kWh was 0.085 €/kWh, considering an average value of the cost of industrial energy in Spain and cost of wine was 0.022 €/L, regarding the information obtained from winemakers.

The optimisation methodology described in Section 2.2 was first applied to the process variables of the continuous fermenter with cell recycling. Table 7 shows the ranges of the process variables that were optimised, the initial fermentation medium concentrations and wine concentration. The time to evaluate the steady state was 72 h, as in the experiments with the pilot fermenter. The ethanol set point for discharge was set at 15 g/L, because, regarding the cell growth model, a lower ethanol concentration would produce low vinegar flows in the continuous fermenter. As reported for semi-continuous processes developed with the pilot fermenter (González-Sáiz et al., 2009), with set points for discharge under 10 g/L, a "re-start" condition was observed at the beginning of each batch, due to the low viability of the medium with low ethanol concentrations. Therefore, the depletion of ethanol in the finisher fermenter would be slower. In fact, set points lower than 10 g/L are used in the industrial plan only when no more than one fermenter is available.

Table 7
Optimisation variables, initial concentrations for each simulation and concentrations of wine used for the optimisation of the continuous fermenter.

Variable	Range	Levels
Optimisation variables		
Overpressure	0–0.78 atm	5
Air	5630–69,434 L h^{-1}	7
Agitation	30–128 rpm	7
Recycling rate	0–0.9	7
Temperature	26–33 °C	3
Concentrations	Initial	Wine
Ethanol (g/L)	50.18	93.74
Acetic acid (g/L)	53.84	0.4952
Ethyl acetate (g/L)	2.029	0.1
Acetoin (g/L)	0.627	0.016
Suspended matter (g/L)	0.35	0.1
Biomass (g/L)	0.35	0

The desirability function used as the optimisation response of the genetic algorithm was:

$$\left[\left(\frac{0.001}{0.001+\Phi}\right)\cdot\left(\frac{F_V}{F_V+5000}\right)\cdot\left(\frac{EA}{EA+1}\right)\right]^{1/3} \quad (48)$$

The economic cost function, Φ worked as a desirability function because a lower cost was obtained when the production of acetic acid was increased with a low energy cost and an optimum ethanol consumption yield. The effect of velocity was also considered with F_V. Ethyl acetate concentration was included as a quality factor, since the sensorial effect of ethyl acetate is typical of high-quality vinegars such as vintaged vinegars or Sherry Vinegars. Although minimum concentration of ethyl acetate is not regulated, ethyl acetate concentrations are usually higher than 1 g/L in vintaged vinegars, while standard vinegars have concentrations under 0.1 g/L, according to information from the vinegar industry. Furthermore, ethyl acetate concentration can be considered as an indicator of the concentration of other volatile esters, which are critical for the flavour of vinegar. Acetoin concentration was not included as a response because it was verified that it hardly varies in simulations, reaching values of around 1 g/L for the continuous fermenter and around 1.2 g/L for the batch fermenter.

The mathematical form of the desirability function was designed to obtain the minimum cost value and the maximum vinegar flow value and ethyl acetate concentration, but there was no objective value, i.e. it did not matter that the optimised values of the function were under 0.6. Table 8 shows the optimised process variables for the continuous fermenter, the values of the responses and the desirability function, the concentration profile of the medium/output flow in the steady state and the concentration of biomass and suspended matter in the output flow, which are lower than the biomass and suspended matter concentration in the fermentation medium, due to cell recycling. These results were obtained by simulation with SEAP. The output flow was used to simulate the feeding and depletion of ethanol in the finisher fermenter. The process variables optimised in the finisher fermenter were overpressure, air, agitation and temperature, with the same ranges and levels as in the continuous fermenter. A similar desirability function was designed to optimise the finisher fermenter:

$$\left[\left(\frac{0.001}{0.001+\Phi}\right)\cdot\left(\frac{r_A}{r_A+5}\right)\cdot\left(\frac{EA}{EA+1}\right)\right]^{1/3} \quad (49)$$

Table 8
Optimisation results for the continuous fermenter.

Optimised variables	
Overpressure (atm)	0.58
Air ($L\,h^{-1}$)	61687
Agitation (rpm)	90
Recycling rate	0.7
Temperature (°C)	30
Optimisation responses	
Economical cost (€/g * L)	0.0269
Vinegar flow ($L\,h^{-1}$)	4232.41
Desirability function	0.2222
Concentration profile of medium produced	
Ethanol (g/L)	14.78
Acetic acid (g/L)	98.66
Ethyl acetate (g/L)	2.01
Acetoin (g/L)	1.05
Suspended matter in fermenter (g/L)	1.90
Biomass in fermenter (g/L)	1.57
Suspended matter in vinegar flow (g/L)	0.57
Biomass in vinegar flow(g/L)	0.47

Table 9
Optimisation results for the batch fermenter.

Optimised variables	
Overpressure (atm)	0.78
Air ($L\,h^{-1}$)	25231
Agitation (rpm)	83
Temperature (°C)	33
Optimisation responses	
Economical cost (€/g * L)	0.0229
r_A ($L\,h^{-1}$)	2.07
Total process time (h)	8.86
Total volume discharged (L)	29957.32
Desirability function	0.2045
Concentration profile of vinegar produced	
Ethanol (g/L)	0.07
Acetic acid (g/L)	116.96
Ethyl acetate (g/L)	2.34
Acetoin (g/L)	1.24
Suspended matter (g/L)	0.66
Biomass (g/L)	0

r_A was calculated as the difference between the final concentration of acetic acid and the concentration of the medium supplied by the continuous fermenter, divided by total process time, which included charge and discharge times. The same comments reported for Equation 56 are applied for this desirability function. Table 9 shows the optimised process variables for the finisher fermenter, the response values and the desirability function and concentration profile of the final vinegar, obtained by simulation with SEAP. In terms of process time, two finishers were required, as designed. The optimised values of the process variables in the continuous and finisher fermenter revealed the importance of overpressure in controlling the volatile compound losses, together with the impact of recycling rate, although values over a limit, 0.7 in this case, did not increase the process rate, due to the limitation of the oxygenation conditions (González-Sáiz et al., 2009). Maximum aeration and agitation values were not reached, since aeration and agitation represented an enhancement of the energy cost, which was not compensated by the slight increase in growth rate, due to the saturation effect and the inhibitory effects as a function of temperature and pressure, as described in Section 3.1.

All in all, the process designed would supply 29957.32 L of vinegar every 8.86 h, with the concentration profile shown in Table 9, which would become 58395.81 L of commercial vinegar with ethanol 0.00° v/v, acetic acid 6° m/v, ethyl acetate 1.20 g/L and acetoin 0.64 g/L. Ethyl acetate concentration would provide a profile closer to a vintage vinegar, while in standard commercial vinegars ethyl acetate concentration is practically negligible. Furthermore, acetoin concentration would achieve not only the minimum concentration established by Spanish regulations, 0.03 g/L, but also the minimum concentration established, for example, for vinegars within Guaranteed Origin "Vinagre del Condado de Huelva", 0.1 g/L. In terms of the data obtained from fermentation processes developed in industrial plant, the standard submerged process with two semi-continuous fermenters and one finisher, equipped with auto aspirant turbines, supplies 28,000 L of vinegar every 30.74 h, with an average acetic acid concentration of 128.10 g/L, residual ethanol 2.37 g/L, ethyl acetate 0.1 g/L and acetoin 0.25 g/L. This final product becomes 59,780 L of commercial vinegar with ethanol 0.14° v/v, acetic acid 6° m/v, ethyl acetate 0.05 g/L and acetoin 0.12 g/L. Therefore, the process designed in this section would improve both the economical yield and the quality of the final product.

4. Conclusions

It has been demonstrated that pressure and temperature have an inhibitory effect on bacterial growth in vinegar production, which is not related to the effect of oxygen transfer. Ethanol concentration and oxygen transfer displayed a saturation effect, which became an inhibitory effect in the case of ethanol concentration when pressure and temperature were enhanced. In the case of oxygen transfer, this inhibitory effect did not appear under the maximum aeration and agitation values reached, but the saturation effect showed that it could appear in stronger oxygenation conditions. Finally, the increase in pressure and temperature and the decrease in ethanol concentration enhanced the inhibitory effect of agitation and aeration, which was independent of oxygen transfer.

Considering these results, the scale-up methodology is based on keeping the geometry dimensions of the pilot fermenter and the values of the following variables: aerated mechanical power input, superficial air velocity, temperature, hydrostatic pressure and compound concentrations. These variables maintain the values of $k_La, C^*_{O_2,L}$ and OTR_{max}. Using these parameters, the process variables of the industrial-scale fermenters are scaled down to the values of the pilot fermenter, allowing the application of the model for $\mu_g v$ and the mass transfer models and predicting the behaviour of fermentation in the industrial-scale fermenters.

This paper completes the stages of the scale-up process (Schmidt, 2005), together with previous studies, i.e. process characterization (Garrido-Vidal et al., 2003), model development (González-Sáiz et al., 2008, 2009) and, finally, process optimisation and identification of scale-up parameters reported here. The final result has been the development of a tool to predict the behaviour of the industrial process of acetic fermentation in aerated-stirred fermenters with any industrial scale, designed within a set of dimension rates, and evaluate the economical balance of vinegar production. As an example of the applicability of SEAP, a fermentation process was designed and optimised. In terms of the optimisation methodology, the experimental design and response surface were combined with genetic algorithms using a desirability function as a response.

Finally, the methodology developed in this series of studies can be applied to several aerobic bioprocesses with different aeration and agitation systems. In future research, a user friendly interface will be programmed for SEAP.

Acknowledgements

The authors thank the Spanish Government (Ministerio de Educación y Ciencia, Project No. AGL2003-09138-C04-04), the Autono-

mous Government of La Rioja (Plan Riojano de I+D+I, Projects Nos. ACPI-2004/02 and ACPI-2005) and the University of La Rioja for their financial support.

References

Aiba, S., Humphrey, A.E., Millis, F.N., 1973. Biochemical Engineering, second ed. Academic Press Inc., New York and London.

Betts, J.I., Doig, S.D., Baganz, F., 2006. Characterization and application of a miniature 10 ml stirred tank bioreactor, showing scale down equivalence with a conventional 7 L reactor. Biotechnology Progress 22, 681–688.

Brindley Alías, C., García-Malea López, M.C., Acién Fernández, F.G., 2004. Influence of power supply in the feasibility of *Phaeodactylum tricornutum* cultures. Biotechnology and Bioengineering 87 (6), 723–733.

Buchanan, R.E., Gibbons, N.E., 1984. Bergey's Manual of Systematic Bacteriology, nineth ed. Williams and Wilkins, Co., Baltimore.

Çelik, E., Çalik, P., 2004. Bioprocess parameters and oxygen transfer characteristics in β-lactamase production by bacillus species. Biotechnology Progress 20, 491–499.

Chen, N.H., 1979. An explicit equation for friction factor in pipe. Industrial and Engineering Chemistry Fundamentals 18 (3), 296.

Cramer, A.C., Vlassides, S., Block, D.E., 2001. Kinetic model for nitrogen-limited wine fermentations. Biotechnology and Bioengineering 77 (1), 49–60.

Doehlert, D.H., 1970. Uniform shell designs. Applied Statistics 19, 231–239.

El-Enshasy, H., Kleine, J., Rinas, U., 2006. Agitation effects on morphology and protein productive fractions of filamentous and pelleted growth forms of recombinant *Aspergillus niger*. Process Biochemistry 41, 2103–2112.

Garrido-Vidal, D., Pizarro, C., González-Saiz, J.M., 2003. Study of process variables in industrial acetic fermentation by a continuous pilot fermentor and response surfaces. Biotechnology Progress 19, 1468–1479.

Garrido-Vidal, D., Esteban-Díez, Isabel, Pérez-del-Notario, Nuria, González-Saiz, J.M., Pizarro, C., 2004. On-line monitoring of kinetic and sensorial variables in acetic fermentation by near infrared spectroscopy. Journal of Near Infrared Spectroscopy 12, 15–27.

Gillard, G., Trägårdh, F., 2003. Mixing in industrial Rushton turbine-agitated reactors under aerated conditions. Chemical Engineering and Processing 42, 373–386.

González-Sáiz, J.M., Pizarro, C., Garrido-Vidal, D., 2008. Modelling gas–liquid and liquid–gas transfers in vinegar production by genetic algorithms. Journal of Food Engineering 87, 136–147.

González-Sáiz, J.M., Pizarro, C., Garrido-Vidal, D., 2009. Modelling the industrial production of vinegar in aerated-stirred fermenters in terms of process variables. Journal of Food Engineering 91, 183–196.

Jiménez-Hornero, J.E., 2007. Contribuciones al modelado y optimización del proceso de fermentación acética, Ph.D. Thesis, Department of Computer Science and Automatics, National University of Distance Learning.

Kim, C.H., Rao, K.J., Youn, D.J., Rhee, S.K., 2003. Scale-up of recombinant hirudin production from *Saccharomyces cerevisiae*. Biotechnology Bioprocess Engineering 8, 303–305.

Lee, F.C., Rangaiah, G.P., Ray, A.K., 2007. Multi-objective optimisation of an industrial Penicillin V Bioreactor train using non-dominated sorting genetic algorithm. Biotechnology and Bioengineering 98 (3), 586–598.

Lide, D.R., Frederikse, H.P.R. (Eds.), 1995. CRC Handbook of Chemistry and Physics, 76th ed. CRC Press, Inc., Boca Raton, FL.

Lucasius, C.B., Kateman, G., 1993. Understanding and using genetic algorithms. Part 1. Concepts properties and context. Chemometrics Intelligent Laboratory Systems 19, 1–33.

Lucasius, C.B., Kateman, G., 1994. Understanding and using genetic algorithms. Part 2. Representation, configuration and hybridization. Chemometrics Intelligent Laboratory Systems 25, 99–145.

Luyben, W.L., 2004. Quantitative comparison of temperature control of reactors with jacket cooling or internal cooling coils. Industrial and Engineering Chemistry Research 43 (11), 2691–2703.

Macías, M., Caro, I., Cantero, D., 1996. Optimum operating conditions in closed-system industrial acetifiers (batch operation): a study by computer simulation. The Chemical Engineering Journal 62, 183–191.

Macías, M., Caro, I., Cantero, D., 1997. Optimum operating conditions in closed-system industrial acetifiers (semi-continuous operation): a study by computer simulation. Chemical Engineering Journal 65, 197–201.

Massart, D.L., Vandeginste, B.G.M., Buydens, L.M.C., De Jong, S., Lewi, P.J., Smeyers-Verbeke, J., 1994. Handbook of Chemometrics and Cualiametrics Part A. Elsevier, London.

Mathews, J.H., Kurtis, J.H., 1999. Numerical Methods using MATLAB, third ed. Prentice Hall, Inc., New Jersey, USA.

Nishiwaki, A., Dunn, I.J., 2005. Analyse of acetic acid productivity in a continuous two-stage bioreactor with cell recycling. Journal of Chemical Technology and Biotechnology 80, 371–375.

Papoutsakis, E.T., 1991. Fluid-mechanical damage of animal cells in bioreactor. Trends in Biotechnology 9, 427–437.

Park, Y.S., Toda, K., 1990. Simulation study on bleed effect in cell-recycle culture of *Acetobacter aceti*. Journal of General and Applied Microbiology 36, 221–233.

Perry, R.H., Green, D.W., Maloney, J.O. (Eds.), 2001. Perry's Chemical Engineers Handbook, seventh ed. McGraw-Hill, Singapore.

Reid, R.C., Prausnitz, J.M., Sherwood, T.K., 1987. The Properties of Gases and Liquids, fourth ed. New York, McGraw-Hill.

Schmidt, F.R., 2005. Optimisation and scale up of industrial fermentation processes. Applied Microbiology and Biotechnology 68, 425–435.

Shukla, R., Chand, S., Srivastava, A.K., 2005. Improvement of gibberellic acid production using a model based fed-batch cultivation of *Gibberella fujikuroi*. Process Biochemistry 40, 2045–2050.

Vogel, H.C., Todaro, C.L., 1997. Fermentation and biochemical engineering handbook. Principles, Process Design and Equipment. Noyes Publications, Westiwood (New Jersey).

Wernersson, E.S., Trägårdh, C., 1999. Scale up of Rushton turbine-agitated tanks. Chemical Engineering Science 54, 4245–4256.

Wong, I., Hernández, A., García, M.A., Segura, R., Rodríguez, I., 2002. Fermentation scale up for recombinant K99 antigen production cloned in *Escherichia coli* MC1061. Process Biochemistry 37, 1195–1199.

Wong, I., García, M.A., Rodríguez, I., Ramos, L.B., Olivera, V., 2003. Fermentation scale up for production of antigen K88 expressed in *Escherichia coli*. Process Biochemistry 38, 1295–1299.